Noisy Localization on the Sphere: Planar Approximation

Baoqi Huang
The Australian National University
Canberra ACT 2600, Australia
Email:Baoqi.Huang@anu.edu.au

Changbin Yu
The Australian National University
Canberra ACT 2600, Australia
Email:Brad.Yu@anu.edu.au

Brian D.O. Anderson
The Australian National University
and National ICT Australia Ltd, Locked Bag 8001
Email:Brian.Anderson@anu.edu.au

Abstract—**In real localization systems, noise from hardware and the environment makes it impossible for any algorithms to precisely localize objects, e.g. sensors and targets. Besides that, planar approximation is another source of error when dealing with localization over spherical surfaces, e.g. the surface of the earth, though it is neglected in many algorithms. This work deals with evaluating the error arising from planar approximation in localization problems over spherical surfaces. We characterize the error as arising for two different though related causes, and accordingly introduce concepts of radial error and angular error to account for these. A localization algorithm, based upon a Cayley-Menger Determinantal condition introduced recently for localization problems, is utilized for the analysis, and analytical results are confirmed through a number of simulations. As an end result of the study, we characterize the regions over which a planar approximation will be satisfactory, given an upper bound on the acceptable error it introduces in comparison with treating localization as a task in three-dimensional space.**

I. Introduction

Localization of sensors, targets and etc. has been an area of active research in recent years, [1], [2]. For example, in wireless sensor networks, normally only a fraction of the nodes (anchors) are provided with position information through e.g. the Global Positioning System (GPS), and others (non-anchor sensors, or if confusion will not arise, simply as sensors) need to be localized. In distance-based localization systems, sensors, including anchors, are equipped with some devices to measure inter-node distances. But noise from hardware and the environment is inevitable in practice, which leads to imprecise distance measurements and consequently imprecise localization results. A number of algorithms have been proposed to estimate sensor positions in the noisy case and in [3], [4] errors in the estimates have been studied.

Besides the noise, another issue is dimensionality. As we know, the surface of the earth is approximately spherical and localization over it, termed the spherical localization, is a three-dimensional (3D) localization problem [5], [6]. It is intuitively clear that the relevant part of the surface, if small enough, can be assumed to be flat, and thus two-dimensional (2D) localization algorithms can be used under planar approximation. Some new error is however induced. If applications require high accuracies of sensor positions, the validity of planar approximation should be verified. More generally, it is also relevant to seek guidelines for the applicability of planar approximation, in terms of the relevant surface area of the earth involved and the desired accuracy of the applications.

To understand the issues with planar approximation, a straightforward method is to compare the 2D localization results under planar approximation with the 3D ones for the same sensors. The localization algorithms [7] based on the Cayley-Menger Determinantal (CMD) condition can work in both the 2D and 3D noisy cases, and the extension to the spherical CMD condition [8] only requires as many anchors as the 2D CMD condition to localize a sensor on the surface of the earth. In this paper, we take this recently developed algorithm to generate position estimates based on both a planar approximation and a full 3D localization, and analyze the resulting error between the two estimates. Of course, this analysis in principle could also be modified if other localization algorithms were used. To make this comparison, a simple network is envisaged: one with three anchors and one sensor with unknown position. This can be regarded as a primitive, from which using, e.g., trilateration, a more complex network might be localized. Localization for this simple network is also equivalent to determining the position of a target, given three range measurements to it. Thus, although the planar approximation issue is introduced and analyzed in terms of sensor localization, this work applies in other similar localization problems over spherical surfaces.

The paper is organized as follows: the next section introduces properties of the Cayley-Menger matrix and its determinant, and their use in related localization algorithms. In Section III we evaluate the error from planar approximation. In Section IV we demonstrate analytical results of the error based on CMD conditions. In Section V simulations are described. We conclude this paper in Section VI.

II. Background

Cao et al. [7] have shown that an entity formed from the distances between three anchors and a sensor and these anchors, termed the 2D CMD condition, can be used to formulate certain geometric relations among these distances in the 2D noiseless case. Similarly, an entity is derived in the 3D noiseless case given four anchors and a sensor. This fact can be exploited in the noisy case so that the effect of errors from noise can be reduced, thereby obtaining a better estimate of the sensor position as compared to other approaches. Using

978-1-4244-2957-8/08/$25.00

these ideas, and under the assumption that the earth is a perfect sphere, Yu et al. [8] develop a spherical CMD condition, which localizes a sensor on the surface of the earth with only three anchors (which is less than the four anchors required to apply the general 3D CMD condition) and the center of the earth as a pseudo-anchor.

A. Cayley-Menger matrix

The Cayley-Menger matrix associated with n points in an $m-$dimensional space is defined as [9]

$$M = \begin{bmatrix} 0 & 1 & 1 & \cdots & 1 & 1 \\ 1 & 0 & d_{0,1}^2 & \cdots & d_{0,n-2}^2 & d_{0,n-1}^2 \\ 1 & d_{1,0}^2 & 0 & \cdots & d_{1,n-2}^2 & d_{1,n-1}^2 \\ \vdots & \vdots & \vdots & \vdots & \vdots & \vdots \\ 1 & d_{n-2,0}^2 & d_{n-2,1}^2 & \cdots & 0 & d_{n-2,n-1}^2 \\ 1 & d_{n-1,0}^2 & d_{n-1,1}^2 & \cdots & d_{n-1,n-2}^2 & 0 \end{bmatrix}$$

where $d_{i,j} = d_{j,i}$, $i, j = 0, \ldots, n-1, i \neq j$ is the Euclidean distance between the points p_i and p_j. The following is a the key theorem which we shall use:

Theorem 1: [9] Consider an n-tuple of points $p_0, ..., p_{n-1}$ in m-dimensional space. If $n \geq m+2$ then the $(n+1)\times(n+1)$ Cayley-Menger matrix $M(p_0, ...p_{n-1})$ has rank $m+2$.

Given five points in 3D, this theorem is equivalent to requiring a single relationship among the associated 10 distances, namely, that the determinant of the matrix M is zero:

$$\det\left(M(p_0, p_1, p_2, p_3, p_4)\right) = 0 \tag{1}$$

B. 2D Cayley-Menger Determinantal condition

Suppose that exact distance measurements are available between three anchors and noisy distance measurements between the anchors and a sensor. Cao et al. [7] formulate an objective function summing the squares of the differences between the squares of measured anchor-sensor distances and squares of the distances associated with an estimate of the sensor position. There are three variables in the objective function, namely the three differences. Because of the CMD condition, which must apply to all possible sensor positions, one can conclude that the three variables necessarily satisfy a constraint, a CMD condition, expressible in terms of these three variables. (The same could be done in 3D, given four anchors and four differences in squared distances).

Let p_0 denote a sensor and p_1, p_2, p_3 denote three anchors. d_{ij} is the accurate Euclidean distance between the points p_i and p_j with $i, j = 0, 1, 2, 3, i \neq j$ and $\overline{d_{0i}}$ is the inaccurate distance acquired by noisy distance measurements with $i = 1, 2, 3$. Then

$$\overline{d_{0i}}^2 = d_{0i}^2 - \varepsilon_i \tag{2}$$

for some difference ε_i. The 2D CMD condition described in [7] is an algebraic equality as following:

$$\varepsilon^T A \varepsilon + \varepsilon^T b + c = 0 \tag{3}$$

where $\varepsilon = [\varepsilon_1, \varepsilon_2, \varepsilon_3]^T$; A is a 3×3 matrix; b is a column vector with three entries; c is a scalar. The associated objective function is $\sum_{i=1}^{3} \varepsilon_i^2$. The entries of A, b and c depend on the precise distances between the anchors and measured distances between the anchors and the sensor, which are all known.

Given exact Euclidean distances between three non-collinear anchors and measured distances between a sensor and these anchors, we can form the 2D CMD condition. By minimizing the objective function subject to the constraint (perhaps with Lagrange multiplier methods), 'optimal' values of ε are determined, and then when the measured distances are corrected by these differences, a set of corrected distances allows determination of a unique estimate of the sensor position in the plane determined by the anchors. *Note that the optimal ε_i in general will not be the same as the values of ε_i associated with the true sensor position.*

C. Spherical Cayley-Menger Determinantal condition

Normally, as in [7], at least four anchors are required to localize a sensor in 3D. But Yu et al. [8] point out that if the earth is assumed to be a perfect sphere and the three anchors and the sensor are all on its surface, the center of the earth can be utilized as a pseudo-anchor because the distances from it to the real anchors and the sensor are known, being the radius of the sphere. A necessary requirement however is that the three anchors not lie on one great circle, which would mean that they together with the pseudo-anchor would be coplanar. Thus, we can form a constraint equation with only three real anchors and involving only three differences of squared distances to localize the sensor. The new constraint, termed the spherical CMD condition, is an equality similar to Eqn. (3):

$$\varepsilon^T A^* \varepsilon + \varepsilon^T b^* + c^* = 0 \tag{4}$$

where A^*, b^*, c^* and ε are similar to their counterparts in Eqn. (3). The noisy Euclidean distances between the anchors and the sensor are immediately obtainable from noisy great circle distances using simple geometry. The similarities between Eqn. (3) and (4) will prove convenient for further analysis.

To utilize this localization algorithm, we reiterate the overall assumption as in [8] that *the earth is a perfect sphere and all anchors (apart from the pseudo-anchor), the sensor lie on its surface and the anchors are not on a single great circle.*

III. Evaluation of the Error From Planar Approximation

Under planar approximation, dimensionality is reduced by one and a 3D localization problem transfers to be 2D. Because distances are measured in 3D, even in the noiseless case they do not strictly fulfill 2D geometric constraints which are the basis of a number of 2D localization algorithms, e.g. [2], [7], [10]. In consequence, the localization result is impaired by inaccuracies from the planar approximation, quite apart from any noise. Measuring the difference between localization results for one sensor with and without the planar approximation, namely the Euclidean distance between the two position estimates, defines a metric for the error.

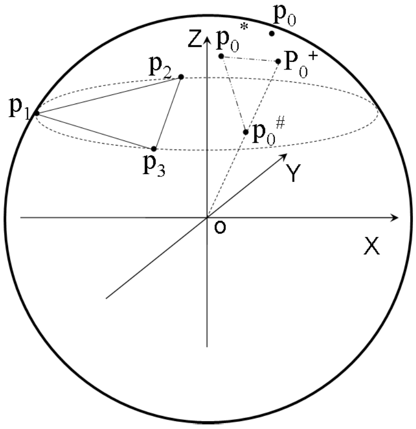

Fig. 1. Localization scenario. The real circle is a great circle of the sphere. The dashed ellipse denotes the boundary of $\mathcal{C}$. The points $p1, p2, p3, p_0, p_0^*$ and p_0^+ are all on the surface of the sphere. The point $p_0^{\#}$ is in the plane $\mathcal{A}$.

Intuitively, the origin of the error is the curvature of spherical surfaces. But it is also affected by particular localization algorithms and any noise in measurements. The metric using this single distance does not reflect certain different aspects of the error and thus we adopt a further way to evaluate it.

In this paper, we use the notation $O(\cdot)$ and $\Theta(\cdot)$ to describe orders of magnitude of quantities. Suppose in particular that f is a function of variable x. For some interval $\mathcal{I}$ of $\mathcal{R}$, typically including 0 or ∞, $f = O(x)$ means for some constant k, there holds $|f| \leq k|x|$ for all x in $\mathcal{I}$; $f = \Theta(x)$ means for some constants k_1 and k_2, there holds $k_1|x| < |f| < k_2|x|$ for all x in $\mathcal{I}$. We can also extend the definition to treat powers of x.

A. Problem model

We illustrate the localization problem of Section II in Fig. 1. The point p_0 represents the sensor to be localized and p_1, p_2, p_3 represent the three anchors. The points $p_0^{\#}$ and p_0^* denote estimated positions of p_0 with and without planar approximation. The assumed plane $\mathcal{A}$ is determined by the points p_1, p_2 and p_3. The points lying both in $\mathcal{A}$ and inside the sphere form a disk $\mathcal{C}$. Note that $p_0^{\#}$ may be inside or outside $\mathcal{C}$. The point p_0^+ is the intersection between the surface of the sphere and the ray starting from the center of the sphere and going through the point $p_0^{\#}$. We remark that while the 2D assumptions return $p_0^{\#}$ which is not in general on the surface of the sphere, a modification to the basic algorithm returning p_0^+ is easily contemplated.

A Cartesian coordinate system is established in Fig. 1 with the center of the sphere as the origin, Z-axis perpendicular to $\mathcal{A}$ and arbitrary orthogonal X- and Y-axes in a plane parallel to $\mathcal{A}$. We designate $\overrightarrow{p}$ as the coordinate vector of the point p in the coordinate system, and $||\overrightarrow{p}||$ for its norm, namely the Euclidean distance from the center of the sphere to the point p. Moreover, $||\overrightarrow{p_0}^* - \overrightarrow{p_0}^{\#}||$ denotes the Euclidean distance between the points p_0^* and $p_0^{\#}$.

We further define the following:

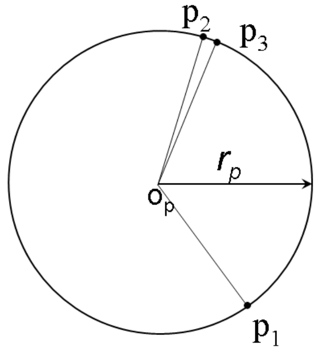

Fig. 2. Nearly collinear anchors. The circle corresponds to $\mathcal{C}$ with O_p as its center and radius r_p.

- $d = \max\{d_{01}, d_{02}, d_{03}, d_{12}, d_{13}, d_{23}\}$, $d_{A_{min}} = \min\{d_{12}, d_{13}, d_{23}\}$ and $d_{A_{max}} = \max\{d_{12}, d_{13}, d_{23}\}$.
- Let $\tilde{\sigma}$ be the great circle distance and σ the Euclidean distance between the points p_0^* and p_0^+.
- r and r_p are the radii of the sphere and $\mathcal{C}$ respectively.
- l is the Euclidean distance between the center of the sphere and the point $p_0^{\#}$.
- h is the distance from the center of the sphere to $\mathcal{A}$.
- W is a 3×3 matrix, the i-th row of which is the coordinate vector of the point p_i, $i = 1, 2, 3$.

$$W = \left[\begin{array}{ccc} \overrightarrow{p_1} & \overrightarrow{p_2} & \overrightarrow{p_3} \end{array} \right]^T \tag{5}$$

The spherical localization procedure cannot be applied if the three anchors are on a common great circle, for then they are coplanar with the fourth pseudo-anchor. Accordingly, we impose the practical restriction that they cannot lie in a plane that is closer than αr to the center of the sphere, i.e.

$$\frac{h}{r} > \alpha \tag{6}$$

Acceptable values for α will be indicated below.

As depicted in Fig. 2, as the least internal angle of the triangle formed by the three anchors, $\angle p_2 O_p p_3$, goes 0, the points p_2 and p_3 tends to overlap, and the three anchors tends to be collinear as well, where the 2D localization procedure does not work. Since $\angle p_2 O_p p_3$ can be approximately expressed by $\frac{d_{A_{min}}}{r_p}$, we impose another practical restriction that the least internal angle of the triangle formed by the three anchors is larger than a small constant β, i.e.

$$\frac{d_{A_{min}}}{r_p} > \beta \tag{7}$$

Acceptable values for β will be indicated below.

As β goes 0, the three anchors tend to be collinear and also coplanar with the center of the sphere. Thus, α and β are not independent. Moreover, when $d_{A_{min}}$ and r_p simultaneously approach 0, it is possible that Eqn (7) holds while h approaches r (certainly larger than αr), but the three anchors gradually overlap, which results in both collinearity and coplanarity of the three anchors and the center of the sphere. In the exceptional case, we restrict the minimal inter-anchor distance $d_{A_{min}}$ to be larger than a small constant ρ, which is easily fulfilled. For instance, $\rho = 0.001$km is reasonable in a real system but sufficient for the constraint.

In fact, both α and β are determined by geometric layouts of three anchors in a localization problem, and together with ρ describe how close the localization problem is to the unacceptable situations, i.e. the three anchors being collinear and the three anchors and the center of the sphere being coplanar. Both of them are suggested by the simulation evidence of Section V as being separately necessary lower bounds.

It is intuitively clear that planar approximation will be much less damaging when $\frac{d}{r}$ is small than when it is large. Simulations presented later show that in fact, e_a (angular error defined in next section) can be beyond 5% when $\frac{d}{r} = 0.314$ since both α and β are well constrained. Hence, we shall restrict attention to values of $\frac{d}{r}$ between 0 and 0.314; equivalently, we are assuming that a planar approximation error exceeding 5% is a sufficient argument not to use planar approximation. Note also that if noise contaminates the measurements, one might well seek to limit the error due to using planar approximation to a level below that associated with the error due to noise. In this case, the acceptable range of $\frac{d}{r}$ could be smaller. To sum up, we shall from now on assume that

$$\frac{d}{r} < 0.314 \tag{8}$$

The measured squared distances $\overline{d_{0i}}^2$ and the associated optimal values of the corrections ε_i with $i = 1, 2, 3$ used in finding the sensor position estimate will be of comparable magnitude to d^2 or less than d^2 respectively. Thus we have

$$\frac{\overline{d_{0i}}^2}{r^2} = O((\frac{d}{r})^2) \tag{9}$$

$$\frac{\varepsilon_i}{r^2} = O((\frac{d}{r})^2) \tag{10}$$

B. Decomposition of the error

As we have mentioned, $||\overrightarrow{p_0}^* - \overrightarrow{p_0}^\#||$ is a metric for the error. In Fig. 1, we notice that two other distances $||\overrightarrow{p_0}^\# - \overrightarrow{p_0}^+||$ and $\tilde{\sigma}$ are like its components along two different directions: 'radial' and 'angular'. $||\overrightarrow{p_0}^\# - \overrightarrow{p_0}^+||$ reflects the aspect of the error from the non-planar characteristic of spherical surfaces, and it can easily be compensated for by a projection step following the 2D localization; $\tilde{\sigma}$ reflects the aspect of the error that directly affects prospective usage of the estimated positions under planar approximation. Thus, the latter one is of importance and we are more concerned with it.

Based on this idea, we decompose the error into two sub-errors: radial error e_r and angular error e_a. Since d indicates the scale of a localization problem, it is appropriate for it to be used to normalize the sub-errors, i.e. dividing the absolute distances by it.

Because σ approaches $\tilde{\sigma}$ when $\tilde{\sigma}$ is small, we use $\frac{\sigma}{d}$ to measure the angular error instead of $\frac{\tilde{\sigma}}{d}$. As to the radial error, we can conclude that $||\overrightarrow{p_0}^\# - \overrightarrow{p_0}^+|| = |r - l|$. Therefore, we define the metrics for the sub-errors:

$$e_r = \frac{|r - l|}{d} \tag{11}$$

$$e_a = \frac{\sigma}{d} \tag{12}$$

IV. Analysis of the Sub-Errors

In this section, we show some analytic results of the sub-errors. Proofs are omitted due to length constraints, and can be obtained from the authors.

A. The radial error

Lemma 1:

$$\frac{r - l}{r} = O((\frac{d}{r})^2) \tag{13}$$

$$\frac{l}{r} = \Theta(1) \tag{14}$$

Based on Eqn. (11) and Lemma 1, we obtain:

$$e_r = O(\frac{d}{r}) \tag{15}$$

which shows that e_r is roughly proportional to d.

B. The angular error

Suppose $\varepsilon^* = [\varepsilon_1^*, \varepsilon_2^*, \varepsilon_3^*]^T$ and $\varepsilon^\# = [\varepsilon_1^\#, \varepsilon_2^\#, \varepsilon_3^\#]^T$ denote the optimal values minimizing the objective functions constrained by the 2D and spherical CMD conditions. We have the following characterization for σ:

Lemma 2:

$$\sigma = \sqrt{Q^T (WW^T)^{-1} Q} \tag{16}$$

where W is as in Eqn. (5) and Q is a column vector with three entries, the i-th ($i = 1, 2, 3$) of which is

$$Q_i = -\frac{r}{l}(r - l)^2 + (\frac{r - l}{l})(\overline{d_{0i}}^2 + \varepsilon_i^\#) + (\varepsilon_i^\# - \varepsilon_i^*) \tag{17}$$

Next, we will record the overbounds of the terms in Eqn. (16) and (17) and with a view to bounding $\frac{\sigma}{d}$. Note that $\overline{d_{0i}}^2 + \varepsilon_i^\#$ is the corrected Euclidean distance between the sensor p_0 and the anchor p_i with the constraint imposed by the 2D CMD condition, and from Eqn. (9) and (10), we obtain

$$\frac{\overline{d_{0i}}^2 + \varepsilon_i^\#}{r^2} = O((\frac{d}{r})^2) \tag{18}$$

Furthermore, we can obtain following lemmas:

Lemma 3:

$$\frac{\varepsilon_i^\# - \varepsilon_i^*}{r^2} = O((\frac{d}{r})^4) \tag{19}$$

Lemma 4:

$$\frac{Q_i}{r^2} = O((\frac{d}{r})^4) \tag{20}$$

Lemma 5:

$$r^2 (WW^T)_{ij}^{-1} = O(1) \tag{21}$$

where $(WW^T)_{ij}^{-1}$ refers to the entry lying in the i-th row and j-th column, with $i, j = 1, 2, 3$.

From Eqn. (12) and Lemma 2, 4 and 5, we can obtain:

Theorem 2: The order of magnitude of the angular error is

$$e_a = O((\frac{d}{r})^3)$$

Theorem 2 reveals that the power in the order of e_a is cubic rather than linear, as was the case for e_r, see Eqn. (15).

V. Simulations

The results of the previous section express errors in terms of orders of magnitude of certain quantities. In this section, we provide simulation evidences for the analytical results which also allows us to make more precise statements about the levels of error. These simulations treat a large number of different localization problems involving three anchors and one sensor, with Matlab used to achieve to determine localization solutions. In all instances, the same problem is solved using both the 2D and spherical CMD conditions. Further details of the simulations are as follows:

- r is 6371.3km, the average radius of the earth.
- the position of every node, namely three anchors and a sensor in each instance, is random, being obtained by generating three spherical coordinates, a constant radial distance r, a random zenith angle and a random azimuth angle. (If the values of parameters d, α, β and ρ are required to fulfill certain constraints, the positions are regenerated until the constraints are fulfilled.)
- noise in a distance measurement is additive independent Gaussian with mean zero and one of several noise levels.

To probe the effects of α and β on the error, we conduct simulations with zero noise. As can be seen from Fig. 3 (a) and (b), it is evident that different scales of $\frac{h}{r}$ result in different levels of the sub-errors except for $\frac{h}{r} > 0.995$: when $\frac{h}{r} \leq 0.1$, both sub-errors are nearly as large as 100% no matter what d is; but when $\frac{h}{r} > 0.995$, they are small and increase with d. The Fig. 3 (c) and (d) show that the instances with large sub-errors (corresponding to the marks on top of the figures) generally have small values of $\frac{d_{A_{min}}}{r_p}$. When $\frac{d_{A_{min}}}{r_p} > 0.1$, both sub-errors are relatively small and increase with d.

Above simulations reflect that for the same value of d small values of $\frac{h}{r}$ and $\frac{d_{A_{min}}}{r_p}$ normally lead to large sub-errors. The principle reason is that a small value of $\frac{d_{A_{min}}}{r_p}$ or $\frac{h}{r}$ implies that the three anchors tend to be collinear in 2D or coplanar with the pseudo-anchor in 3D, which probably causes a large error in the estimated position, and thus the difference between the estimated positions in 2D and 3D, namely the error from the planar approximation, probably rises as well. Therefore, based on the simulations, we suggest that the parameters α and β should be no less than 0.995 and 0.1 respectively to derive acceptable results when applying planar approximation. The equality of $\alpha = 0.995$ indicates $r_p < 636$km, and because $d_{A_{max}}$ denotes the maximal inter-anchor distance which is less than the diameter of $\mathcal{C}$, we have $d_{A_{max}} < 1272$km. On the other hand, the equality of $\beta = 0.1$ indicates that the least internal angle of the triangle formed by the three anchors is larger than $2.86°$. Moreover, when $\frac{h}{r} > 0.995$ and $\frac{d_{A_{min}}}{r_p} >$

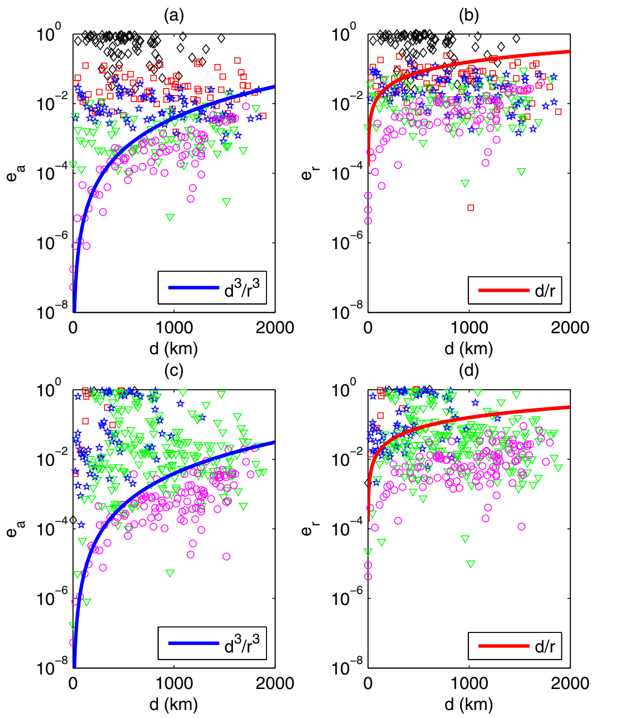

Fig. 3. Simulations with zero noise. In (a) and (b), sub-errors with different scales of $\frac{h}{r}$ are displayed in different shapes: diamond, $0 < \frac{h}{r} \leq 0.1$; square, $0.1 < \frac{h}{r} \leq 0.8$; pentagon, $0.8 < \frac{h}{r} \leq 0.9$; triangle, $0.9 < \frac{h}{r} \leq 0.995$; circle, $0.995 < \frac{h}{r} < 1$. In (b) and (d), sub-errors with different scales of $\frac{d_{A_{min}}}{r_p}$ are displayed in different shapes: diamond, $0 < \frac{d_{A_{min}}}{r_p} \leq 0.0001$; square, $0.0001 < \frac{d_{A_{min}}}{r_p} \leq 0.001$; pentagon, $0.001 < \frac{d_{A_{min}}}{r_p} \leq 0.01$; triangle, $0.01 < \frac{d_{A_{min}}}{r_p} \leq 0.1$; circle, $0.1 < \frac{d_{A_{min}}}{r_p} < \sqrt{3}$. The vertical axes are in logarithm scale.

0.1, both e_a and e_r appear to increase with d and their overall growing trends are close to the curves $\frac{d^3}{r^3}$ and $\frac{d}{r}$ respectively, which also verifies Eqn. (15) and Theorem 2.

Next, we simulate the same instances for zero noise and two different levels of noise, standard deviations of which are $10\% \times d_t$ and $30\% \times d_t$ (d_t denotes the accurate value of the distance to be disturbed. We call the noise levels zero, 10% and 30% for simplicity.) respectively, as depicted in Fig. 4. The parameters α, β and ρ are assigned to be $0.995, 0.1$ and 0.001km respectively. The overall growing trends of e_a and e_r are still close to the real curves, $\frac{d^3}{r^3}$ and $\frac{d}{r}$. Both sub-errors increase slightly with noise from zero to 10% but increase apparently with noise from 10% to 30%.

By the method of trial and error, we can derive three approximate upperbounds of e_a, $\frac{d^3}{5r^3} + \frac{d^2}{5r^2}$, $\frac{d^3}{5r^3} + \frac{d^2}{4r^2}$ and $\frac{d^3}{5r^3} + \frac{d^2}{2r^2}$, for the three levels of noise, corresponding to the dashed curves in Fig. 3. Table I lists some values of these upperbounds of e_a. Because we are more concerned with e_a, the data in Table I give us great confidence in applying the planar approximation due to their small magnitude.

Whether a planar approximation is acceptable is decided by multiple factors, including accuracy requirements on esti-

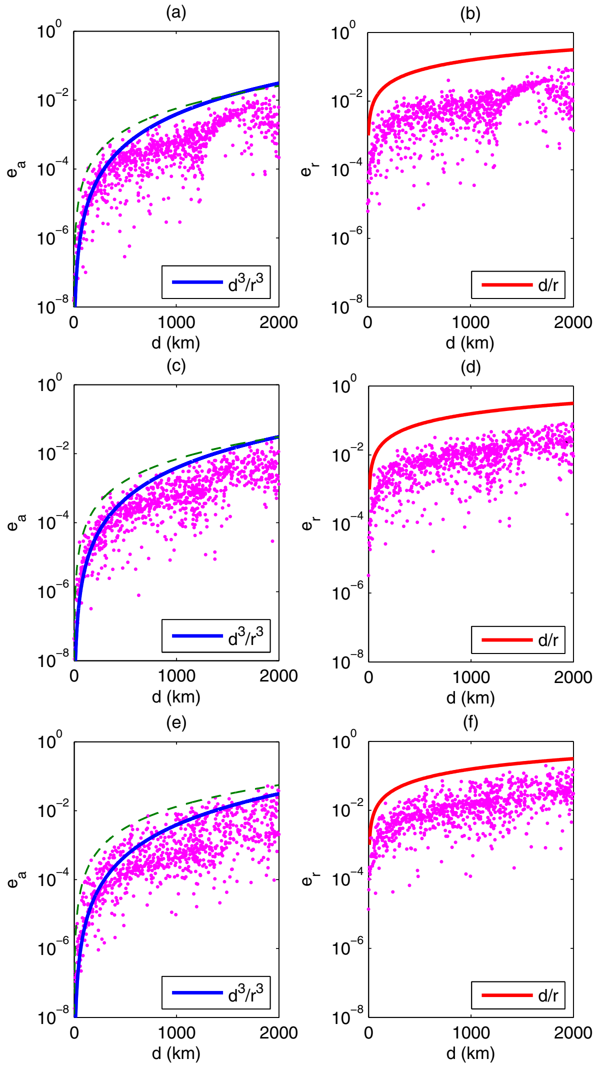

Fig. 4. Simulation for different levels of noise. (a), (c) and (e) show angular error (e_a); (b), (d) and (f) show radial error (e_r). Distance measurements in (a) and (b) are noiseless; distance measurements in (c) and (d) are with 10% noise; distance measurements in (e) and (f) are with 30% noise. Each dot represents a sub-error in one localization instance. The vertical axes are in logarithm scale.

TABLE I
UPPER BOUNDS OF e_a WITH ZERO, 10% AND 30% NOISE

$d(km)$	10	600	1000	2000
zero	$4.93e-5\%$	0.19%	0.57%	2.59%
10%	$6.17e-5\%$	0.24%	0.69%	3.08%
30%	$1.23e-4\%$	0.46%	1.31%	5.55%

mated positions, noise levels in distance measurements and the characteristics of the localization problems described by d, α, β and ρ. Given certain above parameters, we can predict the upperbounds of both sub-errors, comparing the upperbounds with the accuracy requirements on position estimates and uncertainties in distance measurements and then deciding whether the planar approximation is acceptable. For example, provided that in a sensor network the parameters are the same as we have advised and the noise is 10%, e_a will be trivial (less than 0.69%) as long as d is less than 1000km. Otherwise, if sensors are equipped with exact distance measuring devices and then high accuracies on positions are required, or an extremely small value of a parameter is admitted, we should be more cautious in accepting the planar approximation.

VI. CONCLUSIONS

In this paper, we have studied the error from planar approximation in localization problems over spherical surfaces. It is decomposed into two sub-errors: e_r and e_a, and the later one is of importance for it directly affects the perspective usage of estimated positions. In addition, we have identified several critical parameters: d, α, β and ρ, which have significant influences on the error. The parameter d reflects the scale of a localization problem and our work approves that both sub-errors can be characterized if certain constraints are fulfilled. The parameters α, β and ρ define how close a localization problem is to unacceptable situations. We have also analyzed the dependence on these parameters of both sub-errors through a large number of simulations. Guidelines are derived for deciding whether a planar approximation is acceptable in a certain situation.

ACKNOWLEDGMENTS

B. Huang, C. Yu and B.D.O. Anderson are supported by the Australian Research Council under DP-0877562. C. Yu is an ARC Australian Postdoctoral Fellow. B.D.O. Anderson is also supported by National ICT Australia-NICTA. NICTA is funded by the Australian Government as represented by the Department of Broadband, Communications and the Digital Economy and the Australian Research Council through the ICT Centre of Excellence program.

REFERENCES

[1] G. Mao, B. Fidan, and B.D.O. Anderson. Wireless sensor network localization techniques. *Computer networks*, 51:2529–2553, 2007.

[2] A. Savvides, H. Park, and M. Srivastava. The n-hop multilateration primitive for node localization problems. *ACM Mobile networks and applications*, 8:443–451, 2003.

[3] J.N. Ash and R.L. Moses. Relative and absolute errors in sensor network localization. *Acoustics, Speech and Signal Processing*, 2(II):1033–1036, April 2007.

[4] H.A.B.F. Oliveira, E. F. Nakamura, A.A.F. Loureiro, and A. Boukerche. Error analysis of localization systems for sensor networks. In *Proc. the 13th annual ACM international workshop on Geographic information systems*, pages 71–78, New York, NY, USA, 2005.

[5] G.N. Newsam. Locating events on the surface of the sphere from time-of-arrival data. In *Proc. Defence Applications of Signal Processing 2006*, Fraser Island, Queensland, Australia, 2006.

[6] R.O. Schmidt. A new approach to geometry of range difference location. *Aerospace and Electronic Systems, IEEE Transactions on*, AES-8(6):821–835, Nov. 1972.

[7] M. Cao, B.D.O. Anderson, and A.S. Morse. Sensor network localization with imprecise distances. *System and Control Letters*, 55:887–893, 2006.

[8] C.Yu, H. Chee, and B.D.O. Anderson. Noisy localization on the sphere: a preliminary study. In *Proc. the 4th International Conference on Intelligent Sensors, Sensor Networks and Information*, 2008.

[9] L.M. Blunmenthal and B.E. Gillam. Distribution of points in n-space. *The American Mathematical Monthly*, 1(3):181–185, 1943.

[10] D.E. Manolakis. Efficient solution and performance analysis of 3-d position estimation by trilateration. *Aerospace and Electronic Systems, IEEE transactions on*, 32:1239–1248, 1996.